Control of an AUV from Thruster Actuated Hover to Control Surface Actuated Flight

Leo V. Steenson[1], Alexander B. Phillips[1], Eric Rogers[2], Maaten E. Furlong[3], Stephen R. Turnock[1]

[1]Fluid Structure Interactions Research Group, University of Southampton, UK

[2]ISIS Research Group, University of Southampton, UK

[3]National Oceanography Centre, UK

L.V.Steenson@soton.ac.uk

ABSTRACT TITLE

An autonomous underwater vehicle (AUV) capable of both low speed hovering and high speed flight-style operation is introduced. To have this capability the AUV is over-actuated with a rear propeller, four control surfaces and four through-body tunnel thrusters. In this work the actuators are modelled and the non-linearities and uncertainties are identified and discussed with specific regard to operation at different speeds. A thruster-actuated depth control algorithm and a flight-style control-surface actuated depth controller are presented. These controllers are then coupled using model reference feedback to enable transition between the two controllers to enable vehicle stability throughout the speed range. Results from 3 degrees-of-freedom simulations of the AUV using the new controller are presented, showing that the controller works well to smoothly transition between controllers. The performance of the depth controller appears asymmetric with better performance whilst diving than ascending.

1.0 INTRODUCTION

In the past decade the use of autonomous vehicles, both in the air and sea, has increased rapidly. This is due to several factors including the development of control, communications and sensory technologies. However, the main driving factor for the development of these technologies has been to reduce costs of operation and minimize risk to the operators.

As artificial intelligence (AI) technology continues to improve, the opportunity to replace remotely operated vehicles (ROVs) with autonomous underwater vehicles (AUVs) to perform complex missions increases. AI relies heavily on the sensory suite onboard the vehicle to make decisions regarding the mission, but to then perform the manoeuvres to complete the mission requires an equally high performance control system. This work focuses on the development of such a control system to allow an AUV to manoeuvre with similar capability and precision as an ROV but maintain the long range endurance that is typical of a normal AUV. Applications for such a vehicle include; search and inspection of underwater features of interest such as hydrothermal vents, pipelines, and underwater mines.

To achieve this, the vehicle must be able to hover (maintain depth with zero speed) and fly through the water at speed to cover a large distance. Vehicles have been built in the past that offer this capability (Dougherty F., 1988) and (Curtis T.L., 2000) however, the level of control has not been adequate to provide robust control throughout the full vehicle speed range. Between hover and full forward speed is a region where the actuators used to control the vehicle experience extreme non-linearities and uncertainties. The focus of this work is on developing a suitable control system that can maintain full control of the vehicle depth throughout the operating velocity range.

Table 1: Nomenclature

A_H	Area of hull (m^2)
AR	Aspect ratio
A_{SP}	Area of stern-planes (m^2)
a_{sp}	Gradient of lift coefficient against angle of attack (deg^{-1})
B	Buoyancy (N)
$\bar{c}$	Rudder mean chord (m)
C_{LH}	Lift coefficient of hull
C_{LSP}	Lift coefficient of stern-planes
D	Thruster diameter (m)
d	Depth (m)
d_{sp}	Depth set-point (m)
ε	Downwash angle (deg)
e_d	Depth error (m)
e_M	Pitch moment error (Nm)
F_{SP}	Lift force generated by stern-planes (N)
k	Aspect ratio factor
K_{dd}	Thruster actuated depth controller derivative gain
K_{di}	Thruster actuated depth controller integral gain
K_{dp}	Thruster actuated depth controller proportional gain
K_{Mi}	Thruster actuated pitch controller integral gain
K_{Mp}	Thruster actuated pitch controller proportional gain
K_T	Thrust coefficient
$K_{\theta d}$	Flight-style depth controller derivative gain
$K_{\theta i}$	Flight-style depth controller integral gain
$K_{\theta p}$	Flight-style depth controller proportional gain
n	Thruster speed ($rev.s^{-1}$)
n_{VF}	Front vertical thruster demand ($rev.s^{-1}$)
n_{VR}	Rear vertical thruster demand ($rev.s^{-1}$)
S	Control surface span (m)
T	Force generated by thruster (N)
T_d	Thruster-actuated depth controller output (N)
T_M	Thruster-actuated pitch controller output (N)
v	Fluid velocity (ms^{-1})
V_{est}	Estimated flow velocity (ms^{-1})
W	Weight (N)
z_G	Distance between centre of gravity and buoyancy in Z axis (m)
α	Control surface angle of incidence relative to flow (deg)
θ	Pitch angle (deg)
θ_{sp}	Pitch set-point (deg)
ρ	Fluid density ($kg.m^{-3}$)
δ	Control surface angle of incidence relative to body (deg)
δ_{sp}	Stern-plane set-point (deg)

2.0 DELPHIN2 AUTONOMOUS UNDERWATER VEHICLE (AUV)

The Delphin2 AUV, Figure 1, (Phillips A.B., 2010) provides an experimental platform for developing new AUV mission capabilities, planning programs, low-level controllers and for studying the hydrodynamics of AUVs. The vehicle is over-actuated with; two vertical and two horizontal through-body tunnel thrusters, a rear propeller, and four independent control planes. The hull design is a scaled version of that used by Autosub6000 (McPhail, 2010), providing a low drag resistance against forward motion. The combination of the low drag hull and multiple actuators enable Delphin2 to perform hovering ROV type precision manoeuvres as well as long-range survey type missions.

Table 2: Delphin2 AUV Specification

Parameter	Value
Length (m)	1.96
Max. Diameter (M)	0.254
Slenderness Ratio (L/D)	7.72
Weight in Air (kg)	53
Max. Speed (m/s)	2
Min. Speed (m/s)	- 0.4
Max. Depth (m)	50
Dive Rate (m/s)	0.2
Hotel Load (W)	50
Range (km)	20 (estimate)
Operational Time (hrs)	8
Weight – Buoyancy (N)	-7

Figure 1: Delphin2 Autonomous Underwater Vehicle

3.0 MANOEUVERING ACTUATORS

The Delphin2 AUV, like most AUVs, is designed to be positively buoyant. This is a fundamental safety feature so that if there is a systems failure the vehicle will reach the surface and can be easily recovered. To overcome this buoyancy, an equal and opposite force is required. The sum of forces generated by the four thrusters, four control surfaces, the rear propeller and the vehicle hull is used to achieve this. A

control system is required to regulate the magnitude of force developed by these actuators during operation. Although there are actuators fitted to control heading, the focus of this work will concentrate on the actuators used to control the vehicle in the vertical (depth) Z axis.

3.1 Control Surfaces and Propeller

The tail section of the AUV comprises of a rear propeller and four control surfaces. The propeller, Figure 2, is used to provide forward propulsion for the AUV and is driven by a 50W brushless DC motor and the rotational torque is transmitted through the pressure vessel using a magnetic coupling. The four control surfaces are identical and independently operated, Figure 2. These use the NACA-0014 foil profile, Table 3. The angle of incidence relative to the body frame, δ, of each control surface is adjusted using a linear actuator within the sealed tail section pressure vessel. The force of the linear actuator is translated into rotational torque using a simple slider crank mechanism and this torque is then transferred to the control surfaces via a magnetic coupling. The use of a magnetic coupling instead of a shaft seal greatly improves the reliability due to a decreased risk of leakage.

Table 3: Control surface specification

Foil profile	NACA-0014
Max rudder angle	$\pm 30^{o}$
Foil area	8.4×10^{-3} m^2
Mean chord $\bar{c}$	0.104 m
Mean span S	0.0815 m
Mean root gap	0.01 m

Figure 2: Tail section of the Delphin2 AUV

The control surfaces are used for medium to high speed manoeuvres (0.4 to 2ms^{-1}). To overcome the vehicles buoyancy the control system maintains a negative pitch (nose down) using the horizontal control surfaces. This negative pitch generates lift across the AUV hull that is equal opposite to the AUVs buoyancy. As the lift force generated by both the control surfaces and the hull is proportional to flow velocity squared, at low speeds (0 to 0.4 ms^{-1}) the control surfaces are unable to generate sufficient pitching moment to maintain the negative pitch, this is due to the Chinese effect (Burcher, 1994a). During operation at low speeds, the AUV relies upon the tunnel thrusters for manoeuvring and to overcome the vehicles positive buoyancy.

Control of the propeller motor, and the linear actuators used for the control surfaces, is performed by

dedicated electronics within the tail section. These electronics provide feedback to the central computer of the electrical power of the propeller motor, the propeller speed and the position of the linear actuators.

3.2 Through-Body Tunnel Thrusters

The Delphin2 AUV is fitted with two vertical and two horizontal through-body tunnel thrusters, Figure 3. The vertical thrusters generate forces and moments in the Z axis and Y axis respectively, therefore the vertical thrusters are used for depth and pitch control. The tunnel thrusters are used to manoeuvre the vehicle from -0.3 to 0.6 ms^{-1}.

The four blades have a diameter of 70mm and has a pitch ratio of 1.4 at 70% of the propeller radius. The propeller design is a scaled version of a 250 mm diameter thruster (Abu Sharkh, 2003). The thruster units are fitted within 70mm diameter Perspex tunnels and the blades are driven by an externally fitted 250W brushless DC motor that drives permanent magnets which are fitted to the propeller unit. This design enables a very small central hub of the propeller thus maximizing the area of the foil sections. It also means that there are no dynamic seals thus the thruster reliability is improved.

The electronics used to drive the individual thrusters use sensorless control (TSL, 2011) to regulate the thruster speed. Thruster speed demands are provided to the electronics from the central AUV computer via RS-232 serial communication and feedback of the thruster speed, electrical voltage and current is also provided.

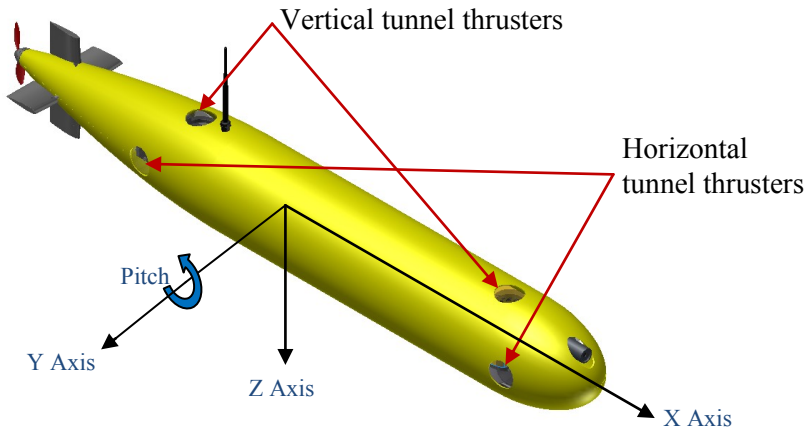

Figure 3: Location of the through body-tunnel thrusters

4 ACTUATOR PERFORMANCE

Before continuing with the design of a control system it is important to first quantify the performance of the actuators and the hull.

4.1 Propeller

There is no direct velocity measurement when the vehicle is submerged, however it is possible to measure the vehicle speed whilst operating on the surface using GPS. Empirical speed response data from operations on the surface have been used to formulate a transient dead-reckoning system within the AUV software. This provides an estimation of the vehicle speed using the measured propeller speed and other vehicle states such as pitch and dive rate. The derivation of the dead-reckoning system is beyond the scope of this work.

4.2 Control Surfaces

To model the lift force generated by the stern plane control surfaces, F_{SP}, a quasi-steady model will be used:

$$F_{SP} = \frac{1}{2}\rho v^2 A_{SP} C_{LSP} \quad [1]$$

For this work, the 2D lift coefficient has been calculated using the computational fluid dynamics software XFOIL (Drela, 1989). The mean slope, a_{SP}, of lift coefficient against angle of incidence (α) is calculated as 0.1 per degree. This simulated data is for a NACA-0014 foil operating in perfect conditions and with infinite span. Thus in reality the performance will differ slightly. For a real foil with finite span the aspect ratio needs to be taken into account. The effective aspect ratio, AR, can be calculated as:

$$AR = k\,S/\bar{c} \quad [2]$$

For a foil with zero root gap (gap between the root of the foil and the hull) the value for k is taken to be 2 however the average gap on the Delphin2 AUV is 10mm. This corresponds to a root gap/mean chord ratio of 0.1 and thus an aspect ratio factor of 1.5. For this work it can be assumed that the aspect ratio does not change substantially between the different control surfaces (Molland, 2007) therefore the aspect ratio is taken as 1.18.

The result of the effective aspect ratio can be determined by assuming it has a flow-straightening effect such that the effective angle of attack, α, is reduced by an angle ε:

$$\varepsilon = \frac{C_{LSP}}{\pi . AR} \quad [3]$$

Thus the lift coefficient for a given angle of incidence becomes:

$$C_{LSP} = a_{sp}(\alpha - \varepsilon) = a_{sp}\alpha\left[\frac{2\pi}{1 + (2/AR)}\right] \quad [4]$$

The lift coefficient is calculated using the stern plane incidence angle relative to the incoming flow. This is not the stern plane angle relative to the vehicle but instead the angle that the flow approaches the stern plane. For the purposes of depth control when the pitch of the vehicle will be varying, it can be assumed that the angle of incidence, α, can be estimated as:

$$\alpha = \delta - \theta \quad [5]$$

For the stern planes, the quasi-steady lift force can be calculated using equations [1], [4], and [5]. The interaction between the stern planes and the free surface or hull is not taken into account. The strongest non-linearity that the control system needs to take into account is that the lift generated by the control surfaces is proportional to flow velocity squared. As the velocity of the flow is not directly measured, inaccuracies in the velocity estimated can create large uncertainties in the control algorithm. Another non-linearity that is not modelled here is the occurrence of stall, when the angle of attack of the control surface or hull exceeds a critical angle dependant upon the physical shape and flow conditions. When stall occurs the lift generated by the foil decreases suddenly whilst drag increases.

4.3 Thruster Model

A quasi-steady model of the thrusters used on Delphin2 is developed in (Steenson L.V., 2011) using equation [6]. Experimental results of thrust against $\rho n^2 D^4$ are plotted in Figure 4, resulting in a K_T value of 0.46. As can be seen the fit is linear and so it is probable that it will work satisfactorily with a linear controller such as a proportional integral controller (PID).

$$T = K_T \rho n^2 D^4 \quad [6]$$

Previous work, (Palmer A.R., 2009a) and (Saunders A., 2002), has shown that the effective thrust produced by through-body tunnel thrusters on AUVs is a nonlinear function of many variables such as; thruster jet speed, vehicle speed and vehicle orientation. Figure 5 plots data from (Palmer A.R., 2009a) where tests on thruster performance were conducted on a vehicle design similar to Delphin2. Here the effective thrust acting on the AUV at different thruster and vehicle speeds have been normalised by the thrust produced at zero forward speed, resulting in the value Kf. As the speed ratio increases the normalised thrust decreases substantially. This non-linearity is not unique to AUVs and is well documented to effect ships operating with bow thrusters at speed (Karlikov, 1998).

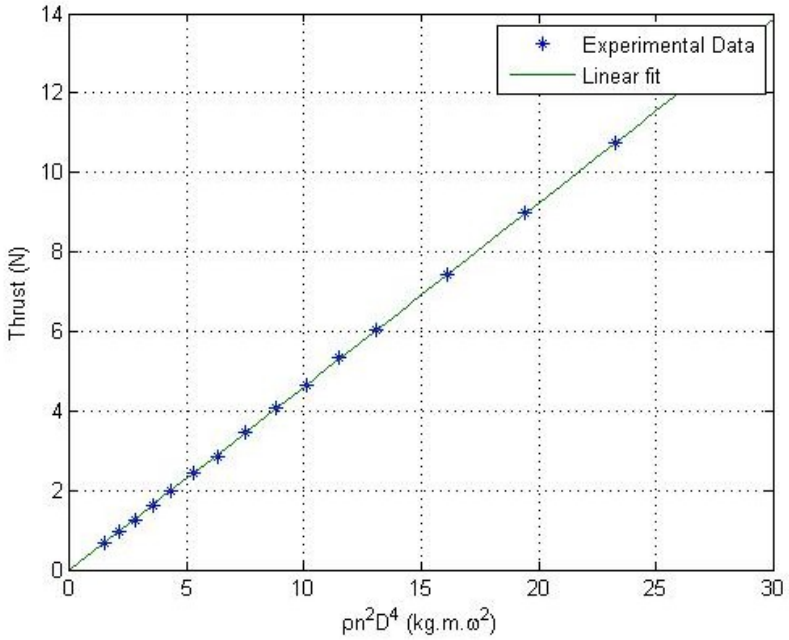

Figure 4: Thrust values from experimental data plotted against $\rho n^2 D^4$.

The cause of this undesirable non-linearity is due to changes in magnitude and location of pressure across the vehicle hull, Figure 6. These variations are a result of the interaction between the thruster jet and the flow around the vehicle due to the vehicle speed. Anti-suction tunnels (AST) have been used on ships to help reduce this differential pressure across the hull and have been shown to improve thruster efficiency during forward speed operation (Salvage, 2011).

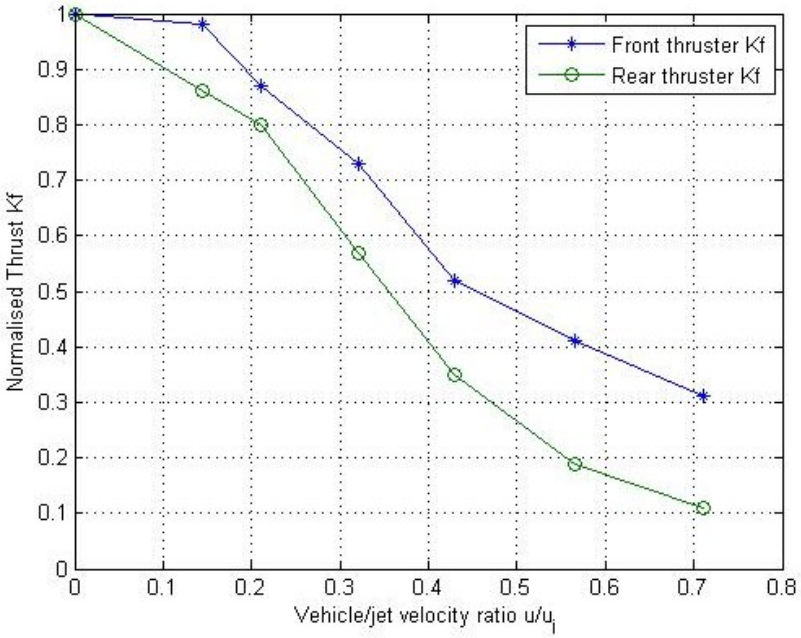

Figure 5: Normalized thrust against forward speed (Palmer A.R., 2009a).

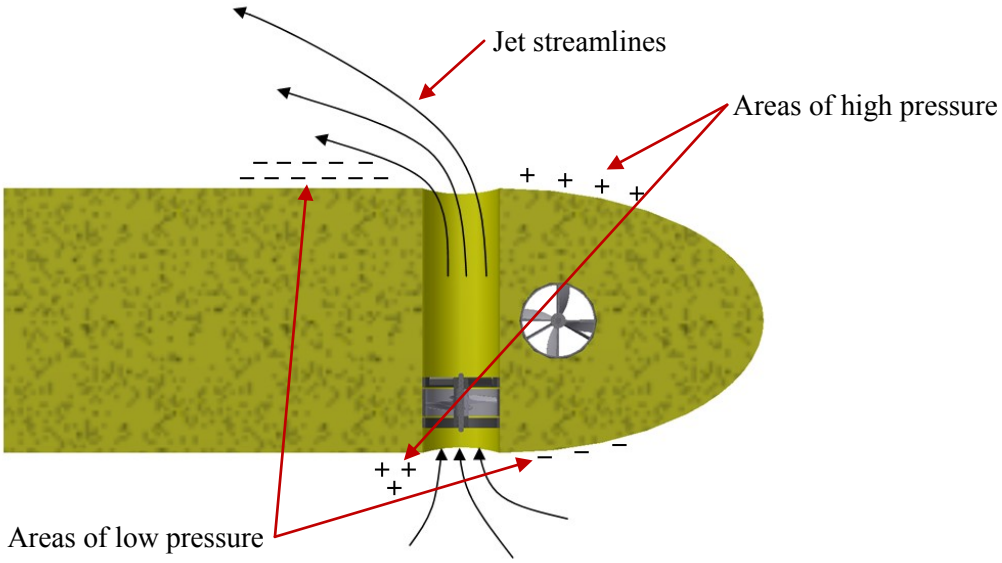

Figure 6: Illustration of pressure distribution across the AUV hull causing a reduction in effective thrust.

4.4 Hull

Although not technically an actuator, the hull will be discussed here as it has a dominant influence on the vehicles manoeuvring capability. The lift generated by the AUV hull is calculated using the same equation as used for calculating the lift from the control surfaces, thus:

$$F_H = \frac{1}{2}\rho v^2 A_H C_{LH} \quad [7]$$

The performance of the hull cannot be simulated accurately using 2D CFD software as used for the stern

planes. Instead, the lift coefficient is taken from experimental data of the Delphin2 AUV at a steady speed, pitch and depth. The lift coefficient value for the hull is taken as 0.011 per degree of pitch.

When operating during flight style, the AUV uses the lift generated by the hull to overcome the vehicles buoyancy. Control of the magnitude of this lift is performed using the control surfaces discussed in section 4.2. As the lift from the hull and control surfaces share the same equation form, so too do they share the same non-linear effects as discussed at the end if section 4.2.

5 CONTROL SYSTEM

The depth control system used on the Delphin2 can be separated into two separate algorithms; one for thruster actuated depth control during hover and low speeds, and another for full flight style operation for medium to high speeds. As the performance of the actuators deteriorates outside of their designed operational envelope, there lies a range of speeds that the performance of the actuators is nonlinear and uncertain. This zone is termed the transitional zone. In this paper, the thruster actuated and flight style depth controllers are presented and then an algorithm used to operate the AUV through the transitional zone explained.

5.1 Thruster Actuated Depth Controller

The depth controller used for low speed operations utilises the vertical thrusters and does not take into account the nonlinearities experienced near the surface or during forward vehicle velocity. The controller comprises of a proportional-integral-derivative (PID) controller for depth control [9] and a proportional-integral (PI) controller for pitch control [10]. The force required to overcome the buoyancy is summed with the PID depth controller to help linearise the system. Any inaccuracy of the stated buoyancy force will be compensated for by the integral component of the algorithm. The depth controller uses the linear depth error and the pitch controller uses the pitching moment error, [8]. The outputs from the depth and pitch controllers are summed (according to moment direction) and then the required thruster speed for each thruster is calculated using the inverse of the thrust equation, [11]. The use of the inverse thruster equations enables the controller to be easily designed as the controller will request forces in Newtons (N). The thruster speed demands are limited within a positive range of values, thus preventing the vehicle from limit cycling due to the motor dead-band whilst changing direction of rotation.

$$e_d(t) = \left(d_{sp} - d\right), \quad e_M(t) = z_G W\left(\sin\theta_{sp} - \sin\theta\right) \tag{8}$$

$$T_d(t) = K_{dp} e_d(t) + K_{di} \int_0^t e_d(\tau)\, d\tau + K_{dd} m + (W - B) \tag{9}$$

$$T_M(t) = \left[K_{Mp} e_M(t) + K_{Mi} \int_0^t e_M(\tau)\, d\tau\right] \left[L_{T_{VR}} + L_{T_{VF}}\right]^{-1} \tag{10}$$

$$n_{VR} = \left[\frac{T_d(t) - T_M(t)}{\rho K_T D^4}\right]^{0.5}, \quad n_{VF} = \left[\frac{T_d(t) + T_M(t)}{\rho K_T D^4}\right]^{0.5} \tag{11}$$

$$n_{VR} = sat\begin{Bmatrix} 2000 \\ n_{VR} \\ 0 \end{Bmatrix}, \quad n_{VF} = sat\begin{Bmatrix} 2000 \\ n_{VF} \\ 0 \end{Bmatrix} \tag{12}$$

5.2 Flight Style Depth Controller

The flight style depth controller is split into two separate proportional-integral (PI) controllers; one for depth control and the other for pitch control. The depth controller receives the depth error [8] as its input and outputs a desired vehicle pitch, [13]. The PI controller output is summed with a steady state pitch angle required to overcome the vehicles buoyancy at the estimated speed, this is calculated using the

inverse of the hull lift equation [7]. Inaccuracies in the lift equation or stated buoyancy will be compensated by the integral component of the algorithm.

The pitch controller calculates pitch error [8] and outputs a suitable control surface angle to achieve the desired pitch, [14]. Note that in [14] the pitch is added so that the control surface is relative to the estimated flow direction. Both controllers' outputs are divided by the vehicle velocity squared to linearise the hydrodynamic forces, note that the minimum velocity provided to the algorithm is a value greater than zero so as to avoid division by zero. The controllers also have their outputs controlled within saturation limits to ensure vehicle stability and so that it operates within the vehicles mechanical limits, [15].

$$\theta_{sp}(t) = \left[K_{\theta p} e_d(t) + K_{\theta i} \int_0^t e_d(\tau)\, d\tau \right] [V_{est}|V_{est}|]^{-1} + [W - B]\left[\frac{1}{2}\rho A_H \dot{C}_{LH} V_{est}|V_{est}|\right]^{-1} \quad [13]$$

$$\delta_{sp}(t) = \left[K_{\delta p} e_M(t) + K_{\delta i} \int_0^t e_M(\tau)\, d\tau \right] [V_{est}|V_{est}|]^{-1} + \theta \quad [14]$$

$$\theta_{sp} = sat\begin{Bmatrix} 10 \\ \theta_{sp} \\ -30 \end{Bmatrix}, \qquad \delta_{sp} = sat\begin{Bmatrix} 30 \\ \delta_{sp} \\ -30 \end{Bmatrix}, \qquad V_{est} = sat\begin{Bmatrix} V_{est} \\ 0.3 \end{Bmatrix} \quad [15]$$

5.3 Transition Algorithm

In order to control depth throughout the speed range requires that the control system can use both the thrusters and control surfaces together. Operating with both controllers simultaneously without modification would cause the vehicle to become unstable due to the buoyancy being compensated for twice. To enable the use of both controllers requires that the total force in the Z axis is regulated.

First the current measured pitch and estimated velocity are used to predict the lift being generated by the hull, using [7]. This is then subtracted from the thruster actuated depth controller and therefore becomes [16]. The flight-style controller remains unmodified and so the depth controller will transition to operating in flight-style mode as quickly as it is possible. This is beneficial as the power consumption of the thrusters is very high in comparison to the rest of the vehicles actuators, therefore operating in flight-style will enable greater operational endurance.

$$T_d(t) = K_{dp} e_d(t) + K_{di} \int_0^t e_d(\tau)\, d\tau + K_{dd} m + (W - B) - \left[\frac{1}{2}\rho A_H \theta \dot{C}_{LH} V_{est}|V_{est}|\right] \quad [16]$$

5.4 Simulation Results

To test the performance of the control algorithm, simulations have been performed using a 3 degree of freedom model of the Delphin2 AUV. This model includes full transient models of the actuators including the reduction in thruster efficiency, however the model does not account for the possibility of stall of either the hull or control surfaces. Gains for the different controllers have been chosen using trial and error.

Figure 7 presents results from a simulation where the depth set-point is fixed at 2 metres. The speed of the vehicle is then adjusted from 0 to 0.5, 1.0, 0, 1.5 and then to 0 ms^{-1}. In the depth plot, at the top of the

figure, it can be seen that there is a disturbance to the vehicles depth whilst there is acceleration in speed.

It is worth noting that the speed steps (in m/s) from 0 to 0.5, 1 to 0, and 1.5 to zero, present the greatest disturbance to depth control, compared to the other steps. This is likely due to a combination between the reduction in thruster efficiency with speed and the lag associated with the flight-style controller when attempting to generate high angles of pitch.

The main purpose of the transition algorithm is to switch between controllers smoothly. The bottom plot of Figure 7 presents the amount of thrust being generated by the thrusters against time. For the initial dive to two metres depth at the beginning of the simulation, the thrusters are used fully without the assistance of the control surfaces due to the forward speed being zero. At 500 seconds the AUV accelerates to 0.5 m/s, and the magnitude of the thrust is quickly decreased until it reaches zero and the AUV is operating in full flight-style.

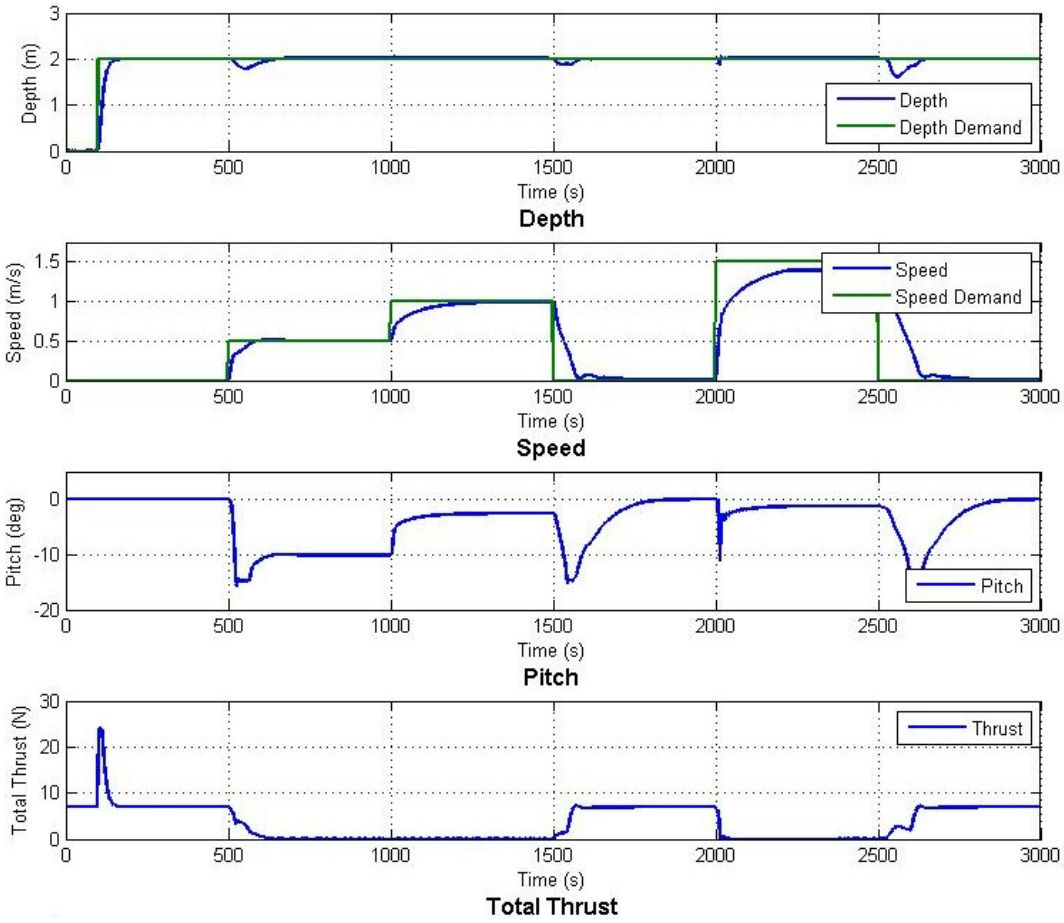

Figure 7: Simulation results of the AUV response to changes in speed set-point at a fixed depth.

Figure 8 presents the results from a simulation where speed of the vehicle is fixed at 1 m/s. The depth demand is varied from 0 to 3, 1, 4, 2 and then 1 metres. As can be seen the performance is asymmetric with good performance diving (increasing in depth) but suffering from a large overshoot during step changes approaching the surface. Whether this overshoot would be acceptable to the operator is dependant upon the specified mission however ideally there should be minimal overshoot. The algorithm does perform well as the thrusters are engaged whenever the overshoots occur to quickly compensate for the insufficient force being generated in the Z axis.

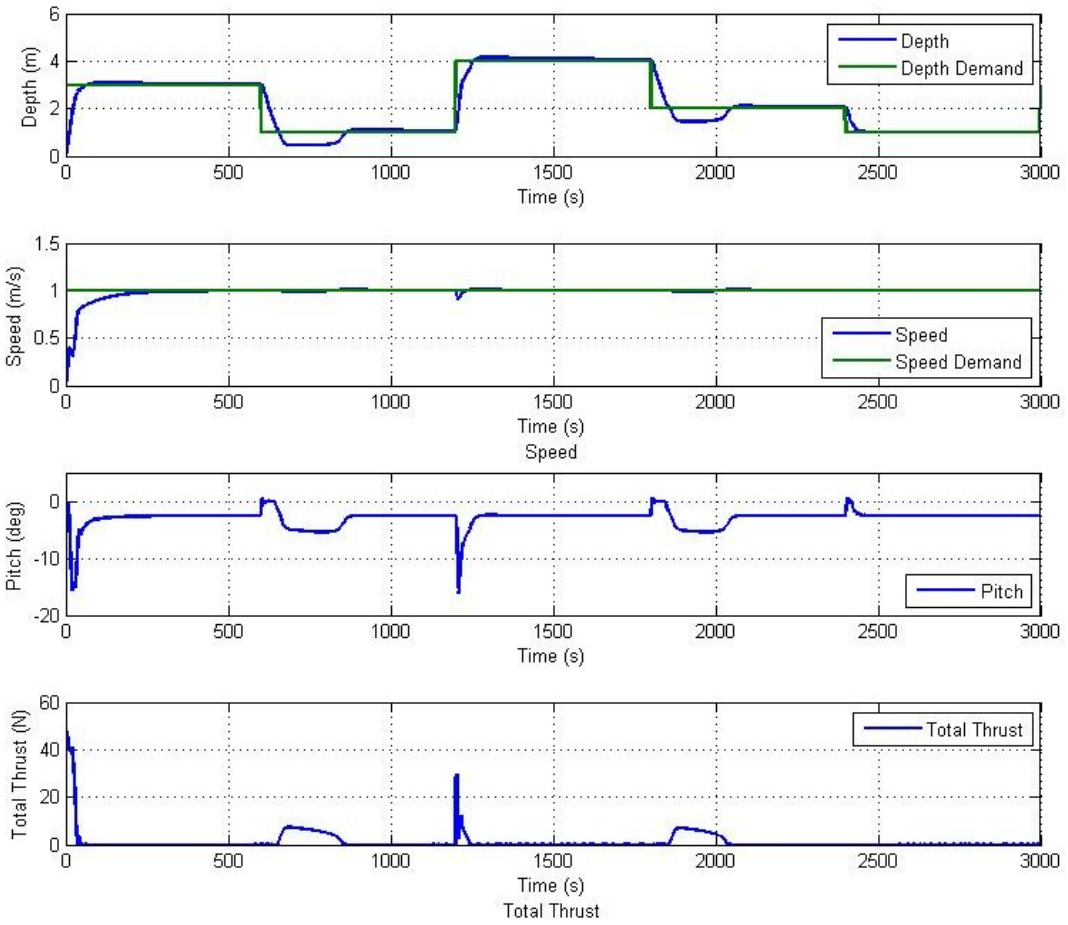

Figure 8: Simulation results of the AUV response to changes in depth set-point at a fixed speed.

6 CONCLUSIONS

The Delphin2 AUV has been introduced as an over-actuated autonomous underwater vehicle. The hull and the performance of the control surfaces, thrusters and propeller have been modelled and the nonlinearities and uncertainties experienced by all the actuators have been discussed.

The control algorithms for the thruster-actuated and the flight-style depth controllers and a method to switch between the two controllers have been presented. Simulations of the full controller operating with different speed and depth demands have been produced. It has been shown that the algorithm works very well at switching between the two controllers throughout the speed range with only small disturbances to the depth observed. The performance of the controller during step changes in depth demand was not fully satisfactory with large overshoots whilst ascending towards the surface.

To fully test the algorithm it is essential that it is tested in the real vehicle rather than simulation. Further study into the AUV system is required to try to eliminate the asymmetric performance experienced whilst performing step changes in depth.

REFERENCES

Abu Sharkh, S. T. (2003). Design and performance of an electric tip-driven thruster. (pp. 133-147). Proceedings of the Institution of Mechanical Engineers, Part M: Journal of Engineering for the Maritime Environment, 217, (3) pp133-147.

Burcher, R. a. (1994a). *Concepts in submarine design.* Cambridge Ocean Technology Series 2, ISBN 10: 0521416817, pp 169.

Curtis T.L., P. D. (2000). C-SCOUT: a general-purpose AUV for systems research . *Underwater Technology, 2000. UT 00. Proceedings of the 2000 International Symposium on*, (pp. 73-77).

Dougherty F., W. G. (1988). An Autonomous Underwater Vehicle (AUV) Flight Control System Using Sliding Mode Control. *IEEE Oceans '88.* Baltimore, MD.

Drela, M. (1989). XFOIL: an analysis and design system for low Reynolds number airfoils. *54*.

Karlikov, V. a. (1998). Some features of body-flow interaction in the presence of transverse jets. *Fluid Dynamics* , 313 - 317.

McPhail, S. (2010). Autosub6000: a deep diving long range AUV. *Journal of Bionic Engineering* , Vols. 6, (1), 55-62.

Molland, A. a. (2007). *Marine Rudders and Control Surfaces.* Butterworth-Heinemann.

Palmer A.R., H. G. (2009a). Experimental testing of an autonomous underwater vehicle with tunnel thrusters. *SMP'09 - First International Symposium on Marine Propulsors*, (pp. 6-12). Trondheim, Norway.

Phillips A.B., S. L. (2010). Delphin2: An Over Actuated Autonomous Underwater Vehicle for Manoeuvring Research. *International Journal of Maritime Engineering* .

Salvage, T. a. (2011, September 13). *Towage-salvage.com.* Retrieved from http://www.towage-salvage.com/files/Chapter_09.pdf

Saunders A., N. M. (2002). The effect of forward vehicle velocity on through-body AUV tunnel thruster performance. *Oceans '02 MTS/IEEE*, (pp. 250 – 259).

Steenson L.V., P. A. (2011). The performance of vertical tunnel thrusters on an autonomous underwater vehicle operating near the free surface in waves . *Second International Symposium on Marine Propulsors*, (pp. 499 - 506). Hamburg, Germany.

TSL. (2011, August 1). *TSL Technology*. Retrieved from http://www.tsltechnology.com/marine/controllers_data.htm